Acta Crystallographica Section D
Biological Crystallography
ISSN 0907-4449

Structure of an archaeal TYW1, the enzyme catalyzing the second step of wye-base biosynthesis

Sakurako Goto-Ito,[a,b] Ryohei Ishii,[b] Takuhiro Ito,[a,b] Rie Shibata,[b] Emiko Fusatomi,[b] Shun-ichi Sekine,[a,b] Yoshitaka Bessho[b] and Shigeyuki Yokoyama[a,b]*

[a]Department of Biophysics and Biochemistry, Graduate School of Science, The University of Tokyo, 7-3-1 Hongo, Bunkyo-ku, Tokyo 113-0033, Japan, and [b]Genomic Sciences Center, Yokohama Institute, RIKEN, 1-7-22 Suehiro-cho, Tsurumi, Yokohama 230-0045, Japan

Correspondence e-mail: yokoyama@biochem.s.u-tokyo.ac.jp

Received 17 July 2007
Accepted 16 August 2007

PDB Reference: TYW1, 2yx0, r2yx0sf.

Wye bases are tricyclic bases that are found in archaeal and eukaryotic tRNAs. The most modified wye base, wybutosine, which appears at position 37 (the 3′-adjacent position to the anticodon), is known to be important for translational reading-frame maintenance. *Saccharomyces cerevisiae* TYW1 catalyzes the tri-ring-formation step in wye-base biosynthesis, with the substrate tRNA bearing N^1-methylated G37. Here, the crystal structure of the archaeal TYW1 homologue from *Pyrococcus horikoshii* is reported at 2.2 Å resolution. The amino-acid sequence of *P. horikoshii* TYW1 suggested that it is a radical-AdoMet enzyme and the tertiary structure of *P. horikoshii* TYW1 indeed shares the modified TIM-barrel structure found in other radical-AdoMet enzymes. Radical-AdoMet enzymes generally contain one or two iron–sulfur (FeS) clusters. The tertiary structure of *P. horikoshii* TYW1 revealed two FeS cluster sites, each containing three cysteine residues. One FeS cluster site was expected from the amino-acid sequence and the other involves cysteine residues that are dispersed throughout the sequence. The existence of two FeS clusters was confirmed from the anomalous Fourier electron-density map. By superposing the *P. horikoshii* TYW1 tertiary structure on those of other radical-AdoMet enzymes, the AdoMet molecule, which is necessary for the reactions of radical-AdoMet enzymes, was modelled in *P. horikoshii* TYW1. Surface plots of conservation rates and electrostatic potentials revealed the highly conserved and positively charged active-site hollow. On the basis of the surface properties, a docking model of *P. horikoshii* TYW1, the tRNA, the FeS clusters and the AdoMet molecule was constructed, with the nucleoside at position 37 of tRNA flipped out from the canonical tRNA structure.

1. Introduction

tRNA molecules contain over 80 types of modified nucleosides and 10–25% of the nucleosides in tRNAs are modified (Grosjean, 2005). In particular, position 34 (the anticodon first letter, or the wobble position) or position 37 (the position next to the anticodon) frequently contains hypermodified nucleosides. Those at position 37 are hypermodified guanosine or adenosine, such as wybutosine (yW), N^6-isopentenyladenosine (i^6A), N^6-threonylcarbamoyladenosine (t^6A) or 2-methylthio-N^6-isopentenyladenosine (ms^2i^6A). When position 36 is A or U, the purine nucleosides at position 37 are almost always hypermodified (Motorin & Grosjean, 2001). The hypermodified nucleosides at position 37 function in translational reading-frame maintenance, as their high hydrophobicity reinforces the codon–anticodon interaction and their modifications prevent them from forming an incorrect Watson–Crick

base pair with the codon's first letter (Urbonavicius *et al.*, 2001; Li *et al.*, 1997; Konevega *et al.*, 2004; Yarian *et al.*, 2002; Murphy *et al.*, 2004).

Furthermore, a lack of yWs in tRNA has some pathological relevance. The eukaryotic $tRNA^{Phe}_{GAA}$ harbours yWs at position 37 in normal cells. However, the $tRNA^{Phe}_{GAA}$ from neuroblastoma cells and ascetic tumour cells lacks the fully modified yWs (Kuchino *et al.*, 1982). In addition, most cells infected with human immunodeficiency virus (HIV) lack yWs in their tRNAs. HIV utilizes the translational frameshifts so that it can produce essential proteins from its small genome. Therefore, the yW-deficient $tRNA^{Phe}_{GAA}$ is considered to be important for the −1 frameshifts at the frameshift signal (Hatfield *et al.*, 1989).

The base of yW contains a tricyclic structure which characterizes the so-called wye bases. yW is the most complex wye base identified thus far and has only been identified at position 37 of eukaryotic $tRNA^{Phe}_{GAA}$. Several types of simpler wye bases have been discovered in the bulk tRNAs of some archaea (Blobstein *et al.*, 1973; Zhou *et al.*, 2004; Waas *et al.*, 2005; Fig. 1), while no wye bases have been found in eubacterial tRNAs (Waas *et al.*, 2005). The wye bases found in archaea include the minimal wye base or 4-demethylwyosine (imG-14), wyosine (imG), isowyosine (imG2) and methylwyosine (mimG) (Noon *et al.*, 2003; McCloskey *et al.*, 2001; Zhou *et al.*, 2004). Of these, imG-14 and imG have also been found in eukaryotes.

Recently, the whole set of genes responsible for yW biosynthesis was identified in *Saccharomyces cerevisiae* (Noma *et al.*, 2006; Fig. 1*a*). The first step is the formation of m^1G37, N^1-methylated G37, which is catalyzed by TRM5 (Waas *et al.*, 2005). The second step is the formation of the tricyclic imG-14 at position 37, which is catalyzed by TYW1. The third, fourth and fifth steps are the addition of the α-amino-α-carboxypropyl group at the C-7 position, methylation at the N-4 position and the addition of a methyl group and a carboxyl group at the C-7 position, which are catalyzed by TYW2, TYW3 and TYW4, respectively.

As m^1G and imG-14 are found in both archaeal and eukaryotic tRNAs, the sequential reactions by TRM5 (m^1G formation) and TYW1 (imG-14 formation) are likely to be common to wye-base formation in archaea and eukaryotes (Fig. 1*b*). Eukaryotic TYW1 is a radical-AdoMet enzyme composed of an N-terminal flavodoxin domain and a C-terminal radical-AdoMet domain. Radical-AdoMet enzymes catalyze various types of reactions utilizing the radical generated by the cleavage of an *S*-adenosyl-L-methionine (AdoMet or SAM) molecule. The common scheme of the radical-AdoMet reactions is shown in Fig. 2 (Layer *et al.*, 2004). An electron supplied by the flavodoxin domain is transferred to the iron–sulfur cluster (FeS cluster) coordinated by the cysteine residues in the radical-AdoMet domain, yielding the most reduced state of the FeS cluster, $[4Fe–4S]^{1+}$. Subsequently, the electron moves to the AdoMet molecule, which is interacting with the FeS cluster, and the reductive cleavage of AdoMet takes place, generating a 5′-deoxyadenosyl radical and a methionine. The reactive 5′-deoxyadenosyl radical abstracts a H atom from the

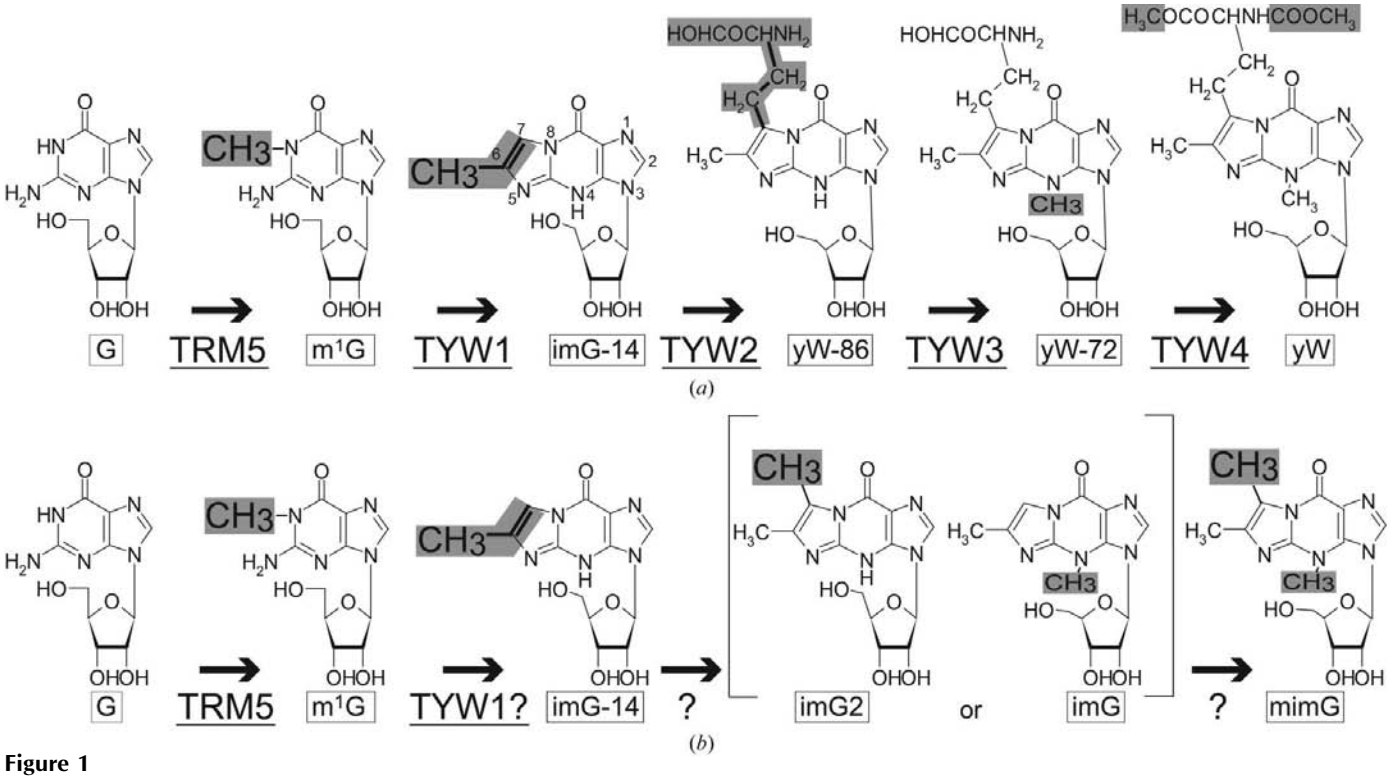

Figure 1
Biosynthetic pathways of wye bases. The grey boxes indicate the moieties added by each enzyme. The names of the wye bases are enclosed in boxes and the enzyme names are underlined. (*a*) The reaction pathway of wybutosine biosynthesis in *S. cerevisiae*. (*b*) The predicted reaction pathway of biosynthesis of wye bases in archaea. The order of imG2 and imG has not been determined.

substrate and the reactions progress. In the reaction catalyzed by TYW1, the tricyclic ring is formed by the addition of two C atoms. Previous studies proposed that the source of the two incorporated C atoms is not methionine and is likely to be a two-carbon molecule, which is still unidentified (Smith *et al.*, 1985).

Here, we report the crystal structure of the archaeal homologue of the *S. cerevisiae* TYW1 C-terminal radical-AdoMet domain from *Pyrococcus horikoshii*. This is the first tertiary structure of a radical-AdoMet enzyme that utilizes a macromolecule as a substrate. The structure revealed that the *P. horikoshii* TYW1 homologue shares a TIM $[(\alpha/\beta)_8]$ barrel structure with other radical-AdoMet enzymes. The functional unit is a monomer, with two FeS clusters. The present structure enabled us to propose the tRNA-recognition mechanism of *P. horikoshii* TYW1.

2. Materials and methods

2.1. Protein expression and purification

The radical-AdoMet domain homologue of *S. cerevisiae* TYW1 was cloned from the *P. horikoshii* genome. The cloned protein (*P. horikoshii* TYW1) was introduced into the pET-11b vector (Novagen) and was overexpressed in an *Escherichia coli* expression system. The native proteins were expressed with Rosetta 2 (DE3) strain in LB medium and the SeMet-derivative proteins were expressed with B834 (DE3) pRARE strain in medium containing selenomethionine instead of methionine. *P. horikoshii* TYW1-expressing cells were lysed and the protein was purified by heat treatment and chromatography on a HiTrap Octyl column (GE Healthcare), a HiTrap SP column (GE Healthcare), a MonoS column (GE Healthcare) and a Superdex200 column (GE Healthcare). The purified protein was concentrated to a final concentration of 18 mg ml^{-1} using an Amicon Ultra filter (Millipore).

2.2. Reconstitution of the FeS clusters

The FeS clusters in the purified protein were reconstituted in an anaerobic chamber as follows. The protein was supplemented with 1 m*M* $Na_2S_2O_4$, 1 m*M* $FeCl_3$ and 1 m*M* Na_2S and kept under anaerobic conditions for 5 h. The excess dithionite, iron and sulfide were removed by passing the protein solution through a PD-10 desalting column (GE Healthcare). The protein fraction was concentrated to 18 mg ml^{-1} and AdoMet was added to a final concentration of 5 m*M*.

2.3. Protein crystallization

Crystals were obtained under several conditions; the best condition was 0.1 *M* MES pH 6.5 containing 12% PEG 20000. The crystallization condition was optimized to 0.1 *M* MES pH 6.0 containing 8% PEG 20000. Crystallization and crystal observation of the FeS cluster-reconstituted protein were performed under anaerobic conditions.

2.4. Data collection and structure determination

P. horikoshii TYW1 crystals were immersed in crystallization solution containing 27.5% MPD as a cryoprotectant and flash-cooled in liquid nitrogen. A single-wavelength anomalous dispersion data set from the SeMet-derivative crystals and a data set from the native crystals were collected at BL5A and NW12 of the Photon Factory (Tsukuba, Japan), respectively. The data set from an FeS cluster-reconstituted crystal was collected with an in-house X-ray generator (Rigaku). The data set was indexed, integrated and scaled with the *HKL*-2000 software (Otwinowski & Minor, 1997). The space group is $P2_12_12_1$, with unit-cell parameters a = 41.9,

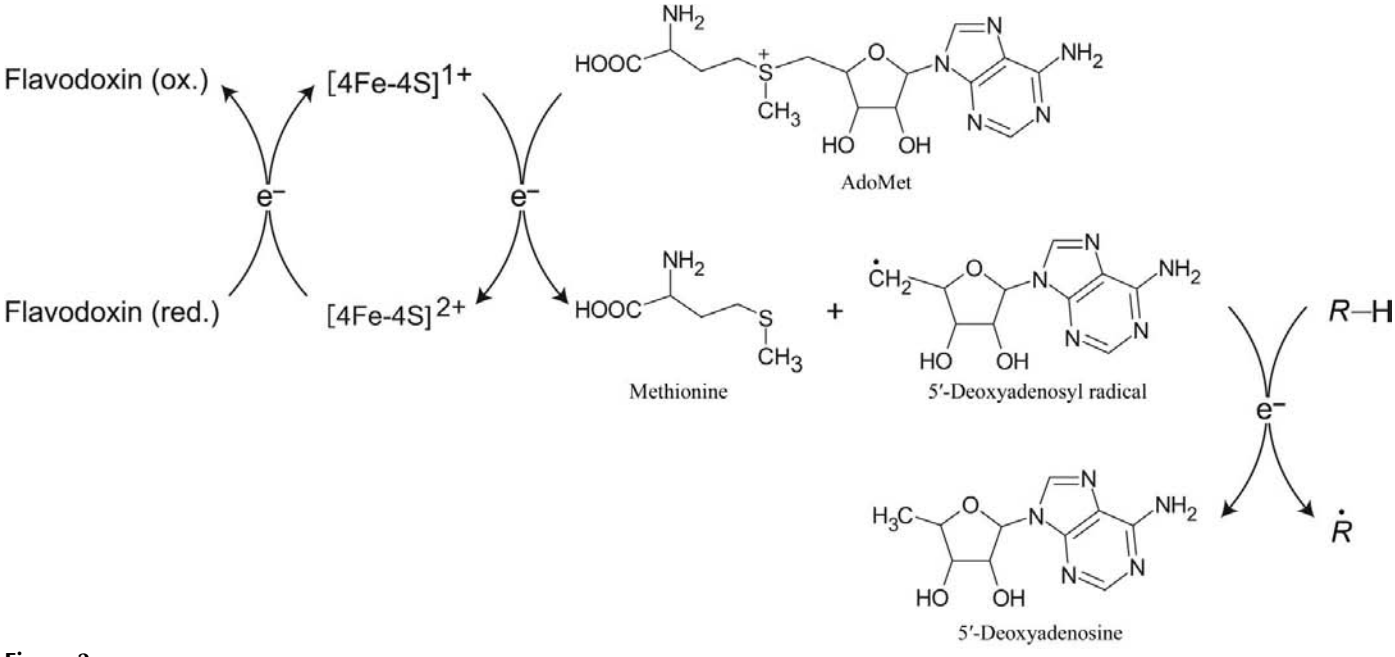

Figure 2
The common scheme of the radical-AdoMet reactions.

Table 1
Data-collection and refinement statistics.

Values in parentheses are for the last shell.

	SeMet, peak	Native	FeS cluster reconstituted
Data collection			
Wavelength (Å)	0.9790	1.0000	1.5418
Resolution (Å)	50–2.2 (2.28–2.20)	50–2.2 (2.28–2.20)	50–4.0 (4.14–4.00)
Space group	$P2_12_12_1$	$P2_12_12_1$	$P2_12_12_1$
Unit-cell parameters (Å)	a = 41.92, b = 60.85, c = 153.81	a = 41.67, b = 60.82, c = 153.26	a = 41.92, b = 59.85, c = 153.66
Observed reflections	254910	105439	46248
Unique reflections	20441	18228	3600
Redundancy	12.6 (8.4)	5.8 (2.6)	12.8 (12.6)
Completeness (%)	99.2 (93.1)	89.2 (51.5)	99.8 (100.0)
Mean $I/\sigma(I)$	24.1 (2.5)	19.6 (2.4)	24.6 (14.5)
R_{sym}† (%)	12.3 (45.1)	9.9 (30.4)	10.6 (20.9)
Phasing			
No. of Se sites found	11 of 16		
Phasing power (ano)	2.14		
FOM (acentric/centric)	0.41/0.12		
Refinement			
Resolution (Å)		50–2.2	50–4.0
Reflections		18175	3571
Mean B value (Å^2)			
Protein		42.9	46.0
Water		56.6	—
R_{work} (%)		19.5	34.4
R_{free} (%)		24.3	39.4
R.m.s.d. bond lengths (Å)		0.012	0.008
R.m.s.d bond angles (°)		1.61	1.36
Ramachandran plot (%)			
Most favoured		86.4	77.9
Additional allowed		12.9	19.6
Generously allowed		0.4	2.5
Disallowed		0.4	0.0

† $R_{sym} = \sum |I_{avg} - I_i| / \sum I_i$.

b = 60.8, c = 153.8 Å. The asymmetric unit contains one monomer. *AUTOSHARP* (Vonrhein *et al.*, 2006) was used for selenium-site picking (*SHELXC*/*SHELXD*; Schneider & Sheldrick, 2002) and phasing (*SHARP*; de La Fortelle & Bricogne, 1997) and *RESOLVE* (Terwilliger, 2000) was used for density modification and automated model building. Phasing of the native crystal data set was carried out by molecular replacement using *MOLREP* (Vagin & Teplyakov, 1997), using the SeMet-derivative model as a search model. The initial model was refined by repetitive cycles of *REFMAC* (Murshudov *et al.*, 1997) and *CNS* (Adams *et al.*, 1997). The final model had an R factor of 19.5% and an R_{free} of 24.3%. Data-collection and refinement statistics are given in Table 1.

2.5. *P. horikoshii* TYW1 and tRNA-binding assay

P. horikoshii $tRNA^{Phe}_{GAA}$ was transcribed *in vitro* by T7 RNA polymerase and was purified using a Resource Q column (GE Healthcare). The *Methanocaldococcus jannaschii* $tRNA^{Phe}_{GAA}$ anticodon stem-loop (5′-GCUGGACUGAAGAUCCAG-3′) was purchased from Dharmacon. Purified RNAs were mixed with various concentrations of purified *P. horikoshii* TYW1 at a final concentration of 38 µ*M*. The mixed solution was analyzed with a 2% agarose gel in 0.5 × TB buffer.

3. Results and discussion

3.1. *BLAST* search for *S. cerevisiae* TYW1 homologues in archaeal and bacterial genomes

We performed a *BLAST* search against all sequenced archaeal and bacterial genomes with the *S. cerevisiae* TYW1 sequence as a query. In every archaeal genome except for that from *Haloquadratum walsby*, a homologue of the C-terminal radical-AdoMet domain of *S. cerevisiae* TYW1 was found. As shown in Fig. 3, these proteins are highly conserved among species, which suggests that they are the orthologues of *S. cerevisiae* TYW1. On the other hand, no proteins homologous to *S. cerevisiae* TYW1 were found in bacterial genomes, which is consistent with the fact that wye bases have not been found in bacteria. A *BLAST* search did not yield any homologues of the N-terminal flavodoxin domain of *S. cerevisiae* TYW1 in archaeal genomes, suggesting that archaea utilize another type of enzyme without flavodoxin as an electron donor for the radical-AdoMet domain. In the *P. horikoshii* genome, the hypothetical protein PH1705 was identified as the homologue of the *S. cerevisiae* TYW1 radical-AdoMet domain. In this report, we refer to the *P. horikoshii* TYW1 homologue simply as *P. horikoshii* TYW1, despite the lack of the flavodoxin domain.

3.2. Overall structure of *P. horikoshii* TYW1

We solved the crystal structure of *P. horikoshii* TYW1 at 2.2 Å resolution. *P. horikoshii* TYW1 is a monomeric protein consisting of 342 amino acids, and residues 11–275 and 282–342 were visible in the crystal structure. As shown in Fig. 4, the overall structure is a half-barrel structure, a variation of the TIM [$(\alpha/\beta)_8$] barrel structure that is common in the tertiary structures of radical-AdoMet enzymes. The half-barrel is composed of six α-helices (α4, α6, α7, α9, α10 and α11) packed against a ten-stranded β-sheet (β1–β10). Other α-helices (α1, α2, α3, α5 and α8) and two long loops (loops β3–α4 and β8–α11) form the walls on both sides of the half-barrel.

From the amino-acid sequence analysis, residues Cys81, Cys85 and Cys88 were predicted to comprise the iron–sulfur cluster (FeS cluster) site (site *A*), because they satisfy the consensus sequence (C*xxx*C*xx*C) of the FeS-cluster site, and they are also perfectly conserved among species, as marked with green dots in Fig. 3. In the crystal structure, their side chains face each other to create the cluster site (Fig. 4). Since the crystallization of *P. horikoshii* TYW1 without the reconstituted FeS clusters was not performed under anaerobic

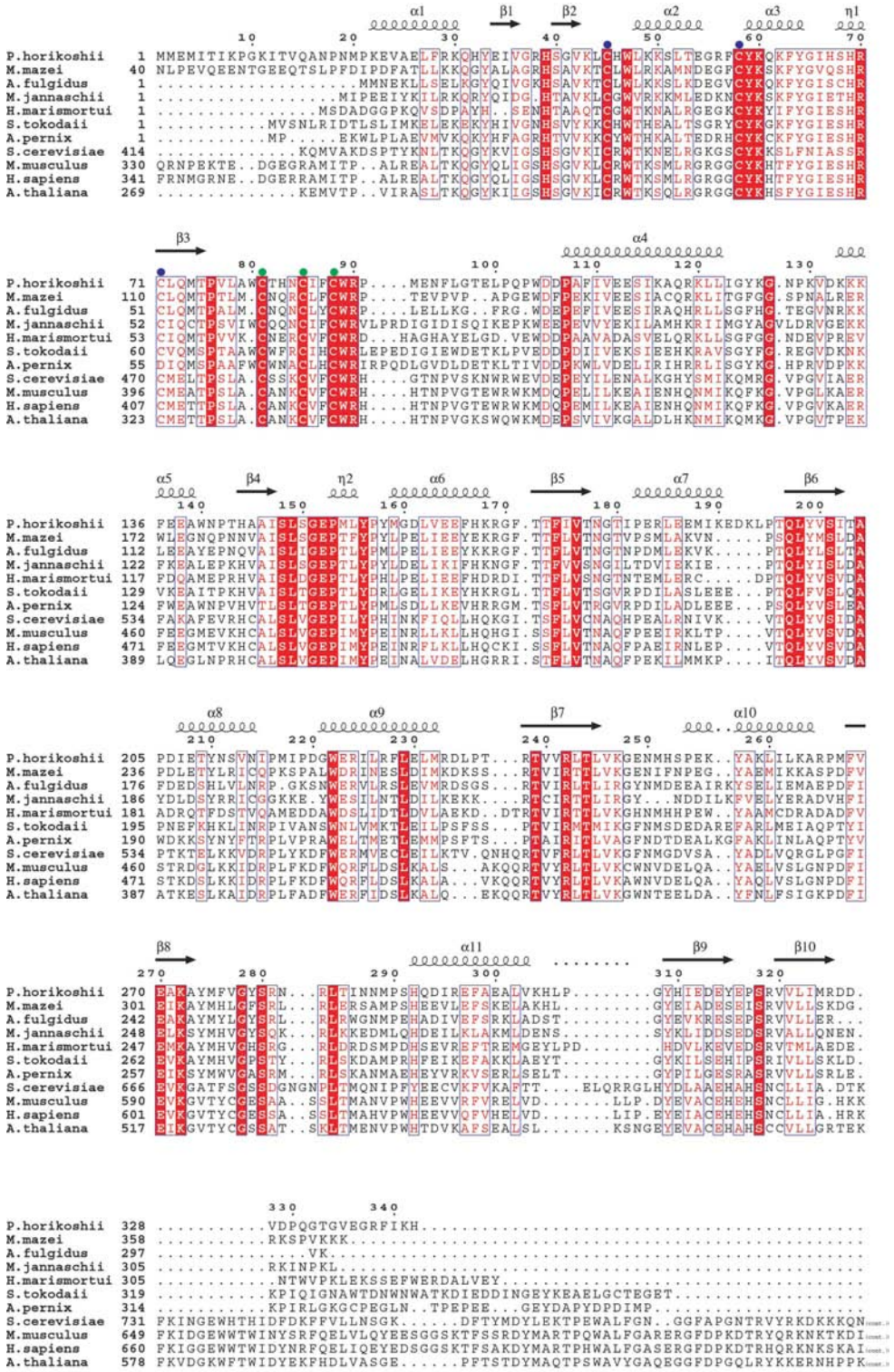

Figure 3
Sequence alignment of *P. horikoshii* TYW1 homologue proteins. The amino-acid sequence of *P. horikoshii* TYW1 is aligned with those of archaeal *S. cerevisiae* TYW1 homologues (*Methanosarcina mazei*, *Archaeoglobus fulgidus*, *Methanococcus jannaschii*, *Haloarcula marismortui*, *Sulfolobus tokodaii* and *Aeropyrum pernix*) and those of eukaryotic *S. cerevisiae* TYW1 homologues (*Saccharomyces cerevisiae*, *Mus musculus*, *Homo sapiens* and *Arabidopsis thaliana*). The secondary structures α-helices, β-strands and 3_{10}-helices are denoted by the Greek characters α, β and η, respectively. The fully conserved residues are highlighted in red boxes and the red amino-acid residues are moderately conserved. The residues participating in the FeS-cluster sites *A* and *B* are marked by green and blue dots, respectively.

conditions, Cys85 and Cys88 seemed to form a disulfide bond in the crystal structure, with a distance between their S atoms of 2.02 Å. However, they may not always form a disulfide bond, as their side chains coordinated the FeS cluster when the clusters were reconstituted into *P. horikoshii* TYW1. The present crystal structure revealed another possible FeS-cluster site (site *B*). Cys45, Cys58 and Cys71 are located close together in the tertiary structure, as shown in Fig. 4, although they are not close in the primary structure. Cys45 and Cys58 are completely conserved in the 41 species examined (as marked with blue dots in Fig. 3). Cys71 is also conserved in 40 out of 41 species, with the only exception being that from *Aeropyrum pernix*. The high conservation rates suggest that site *B* is also functional and indispensable for the catalysis.

To determine whether sites *A* and *B* actually hold the FeS clusters, we reconstituted the FeS clusters in the protein and prepared the crystals anaerobically. The UV–visible spectrum was used to confirm the FeS-cluster reconstitution, as FeS clusters are known to have absorption peaks at 400–460 nm. The prepared protein had absorption peaks at around 450 nm (data not shown), which indicated that the FeS clusters had successfully been reconstituted. Furthermore, the anomalous Fourier electron-density map was calculated using the data collected at a wavelength of 1.54 Å with the in-house X-ray generator. Since the wavelength of the Fe X-ray absorption peak is around 1.743 Å, the Fe atoms also have some anomalous signal at 1.54 Å wavelength. In the map, electron-density peaks were observed at both sites *A* and *B* (Fig. 5). Therefore, we concluded that sites *A* and *B* are actually capable of holding FeS clusters. The sizes of the anomalous peaks

indicated that sites *A* and *B* seemed to contain [4Fe–4S] and [2Fe–2S] clusters, respectively.

3.3. Structural comparison with other radical-AdoMet enzymes

The *P. horikoshii* TYW1 structure is similar to the monomer structures of other radical-AdoMet enzymes, sharing the modified TIM-barrel structure (top panels in Fig. 6). The distinct difference between the radical-AdoMet enzymes is their functional units. *P. horikoshii* TYW1 behaves as a monomeric protein in the crystal structure and in gel-filtration analysis (data not shown). *E. coli* HemN, an oxygen-independent coproporphyrinogen oxidase, is also a monomeric protein (PDB code 1olt; Layer *et al.*, 2003). On the other hand, *Streptococcus aureus* MoaA (PDB code 1tv8), an enzyme involved in molybdenum-cofactor biosynthesis (Hanzelmann & Schindelin, 2004), and *E. coli* BioB, a biotin synthase (PDB code 1r30; Berkovitch *et al.*, 2004), are homodimeric proteins. *Clostridium subterminale* KamA, a lysine-2,3-aminomutase, is a homotetrameric protein (PDB code 2a5h; Lepore *et al.*, 2005).

In addition to the variation in their functional units, the active sites also differ between the determined radical-AdoMet enzyme crystal structures (bottom panels in Fig. 6). It should be noted that one FeS cluster-binding site in the radical-AdoMet enzymes can hold several types of clusters, such as [4Fe–4S], [3Fe–4S] and [2Fe–2S], depending on the available amount of iron or sulfide and the redox potential of the system (Ugulava *et al.*, 2001). One [4Fe–4S] cluster and two AdoMet molecules per monomer were found in the crystal structure of HemN, although it is unclear whether the second AdoMet molecule is involved in the reaction. The crystal structure of MoaA contains two [4Fe–4S] clusters, one AdoMet molecule and one molecule of the substrate GTP per monomer. The crystal structure of BioB contains one [4Fe–4S] cluster, one [2Fe–2S] cluster, one AdoMet molecule and one molecule of the substrate dethiobiotin (DTB) per monomer. The crystal structure of KamA contains one [4Fe–4S] cluster, one AdoMet molecule, the substrate lysine and the enzymatic cofactor pyridoxal phosphate (PLP). We superposed the three cysteine residues that satisfy the consensus C*xxx*C*xx*C sequence in these radical-AdoMet enzymes (consensus clusters; bottom panels in Fig. 6, the superposed clusters are on the left-hand side). This superposition revealed the common arrangement of the components of the active site: a consensus cluster interacts with an AdoMet molecule, the substrate resides next to the AdoMet, and the nonconsensus cluster or the enzymatic cofactor, if there is one, is next to the substrate.

This common arrangement allowed us to model the FeS clusters and the AdoMet molecule in the *P. horikoshii* TYW1 structure, as shown in Fig. 6(*a*). The [4Fe–4S] cluster and the AdoMet molecule of *P. horikoshii* TYW1 were modelled based on the MoaA crystal structure by superposing Cys24, Cys28 and Cys31 of MoaA onto Cys81, Cys85 and Cys88 of *P. horikoshii* TYW1, as the resulting position of the AdoMet did not clash with the *P. horikoshii* TYW1 structure. The [2Fe–2S] cluster was modelled so that it is coordinated by Cys45, Cys58 and Cys71 of *P. horikoshii* TYW1. The positions of the [4Fe–4S] and [2Fe–2S] clusters were refined in accordance with the anomalous densities described above.

3.4. The docking model of *P. horikoshii* TYW1 with the tRNA

Furthermore, we constructed a docking model of *P. horikoshii* TYW1 with the FeS clusters, AdoMet and the

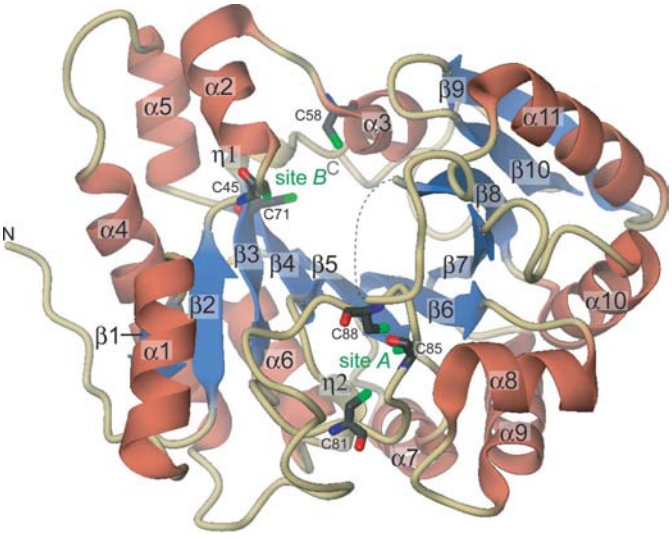

Figure 4
The overall structure of *P. horikoshii* TYW1. The α-helices and β-strands are coloured dark pink and blue, respectively. The 3_{10}-helices are shown in beige and labelled $\eta1$ or $\eta2$. The cysteine residues involved in FeS-cluster formation are shown as stick models with black C atoms and the FeS-cluster sites *A* and *B* are indicated in green letters. The disordered region is shown as a dashed line. This and all subsequent figures in this paper were generated using *CueMol* (http://cuemol.sourceforge.jp).

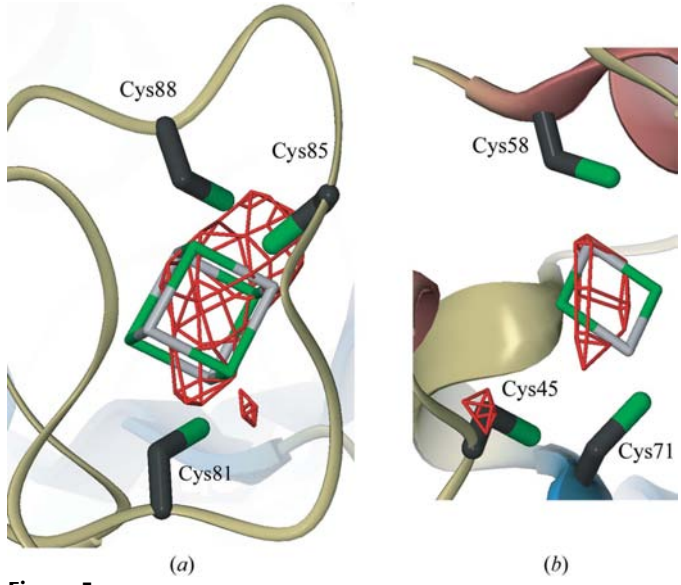

Figure 5
The anomalous map at the FeS-cluster sites. The red mesh is the anomalous Fourier electron-density map calculated using the data collected at a wavelength of 1.54 Å and contoured at 3σ. The modelled FeS clusters are shown as stick models with pale grey Fe atoms and green S atoms. (*a*) and (*b*) show sites *A* and *B*, respectively.

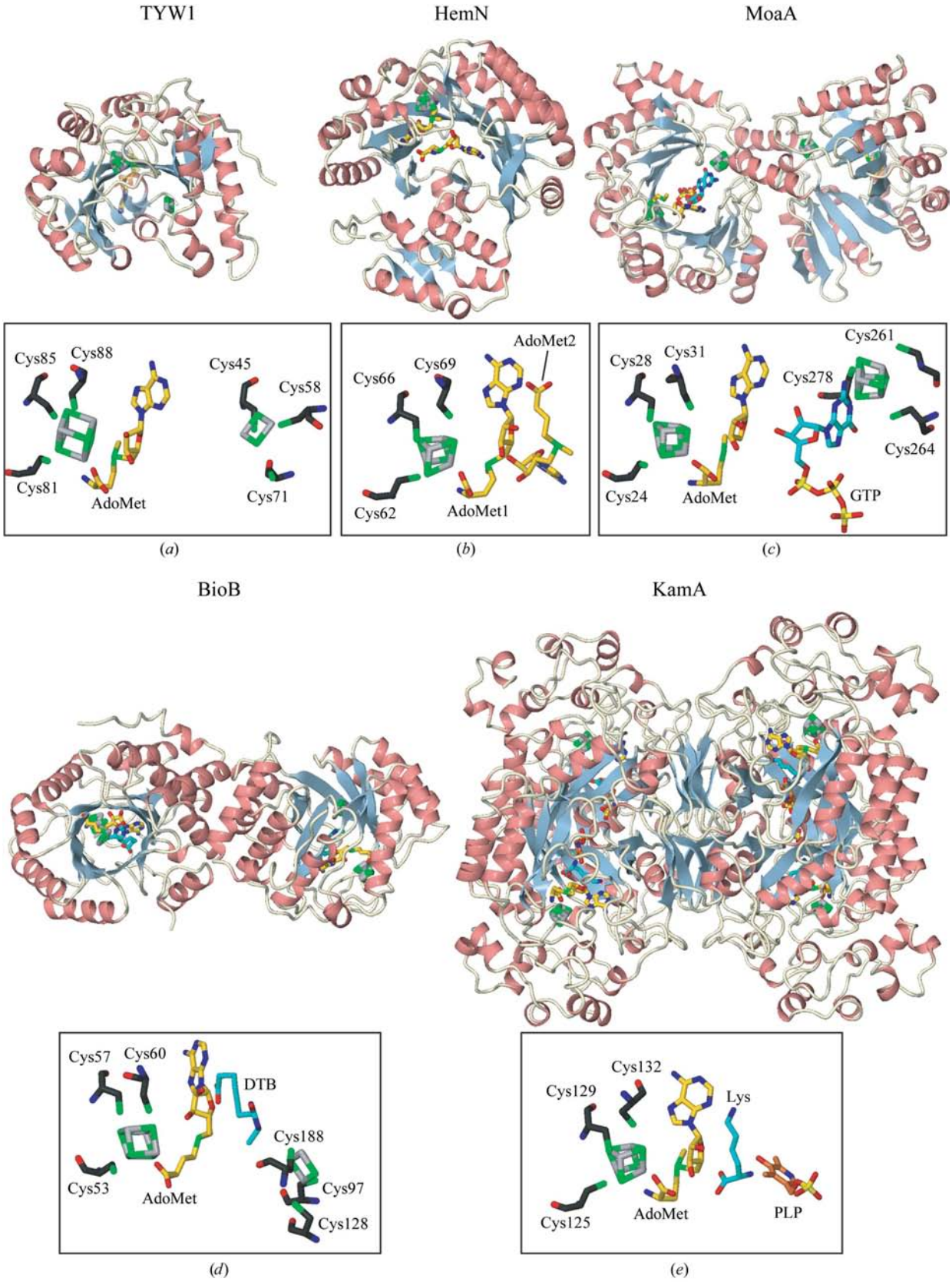

Figure 6
Comparison with other radical-AdoMet enzymes. In (*a*)–(*e*), the top panel shows the overall structure of the functional unit of each radical-AdoMet enzyme, with the FeS clusters, AdoMet, substrate and cofactor shown as stick models with grey and green, yellow, light blue and orange C atoms, respectively. In (*a*) the AdoMet molecule and the FeS clusters are modelled in *P. horikoshii* TYW1. Shown in the bottom panels are close-ups of the active-site components. They are superposed on the cysteine residues comprising the consensus clusters (left-hand side).

tRNA on the basis of the structural properties of the protein (Figs. 7 and 8). We calculated the conservation rates of the *P. horikoshii* TYW1 residues in other TYW1 homologues, and plotted them on the molecular surface of *P. horikoshii* TYW1. As shown in Fig. 7(*b*), the highly conserved residues are localized in the active-site hollow. In addition, an electrostatic potential map of *P. horikoshii* TYW1 revealed that the active-site hollow is highly positively charged (Fig. 7*c*). The positively charged residues are likely to interact with the negatively charged backbone phosphates of the substrate tRNA. The positive charge of the active-site hollow is a unique feature of TYW1 orthologues and is not common to the radical-AdoMet enzymes. Thus, we presume that the highly conserved and positively charged active-site hollow is important in tRNA recognition and catalysis.

The active-site hollow occupied by the FeS clusters and the AdoMet molecule still has sufficient space to accommodate one nucleoside. Therefore, it can be presumed that the tRNA anticodon stem-loop lies on top of the active-site hollow, with the nucleoside at position 37 flipped out from the canonical anticodon stem-loop structure. We chose *S. cerevisiae* $tRNA^{Phe}_{GAA}$ for the starting model, as yW has been identified at position 37 of eukaryotic $tRNA^{Phe}_{GAA}$. We modified the nucleoside at position 37 of the starting tRNA model into m^1G, the substrate for *P. horikoshii* TYW1. m^1G37 is flipped out to reside at the catalytic centre between the AdoMet molecule and the nonconsensus cluster (Fig. 8*c*), in accordance with the common arrangement of the active-site components in the radical-AdoMet enzymes (Fig. 6). Simultaneously, we ensured that the tRNA body did not clash with *P. horikoshii* TYW1. The resulting model has good consistency with the electrostatic state of the *P. horikoshii* TYW1 surface (Fig. 8*a*). As described above, the carbon donor for TYW1 is considered to be an unidentified two-carbon molecule. Thus, this two-carbon molecule may participate in the active site. Referring to the position of the cofactor PLP in the KamA structure (Fig. 6*e*), the two-carbon molecule may reside between m^1G37 and the nonconsensus cluster.

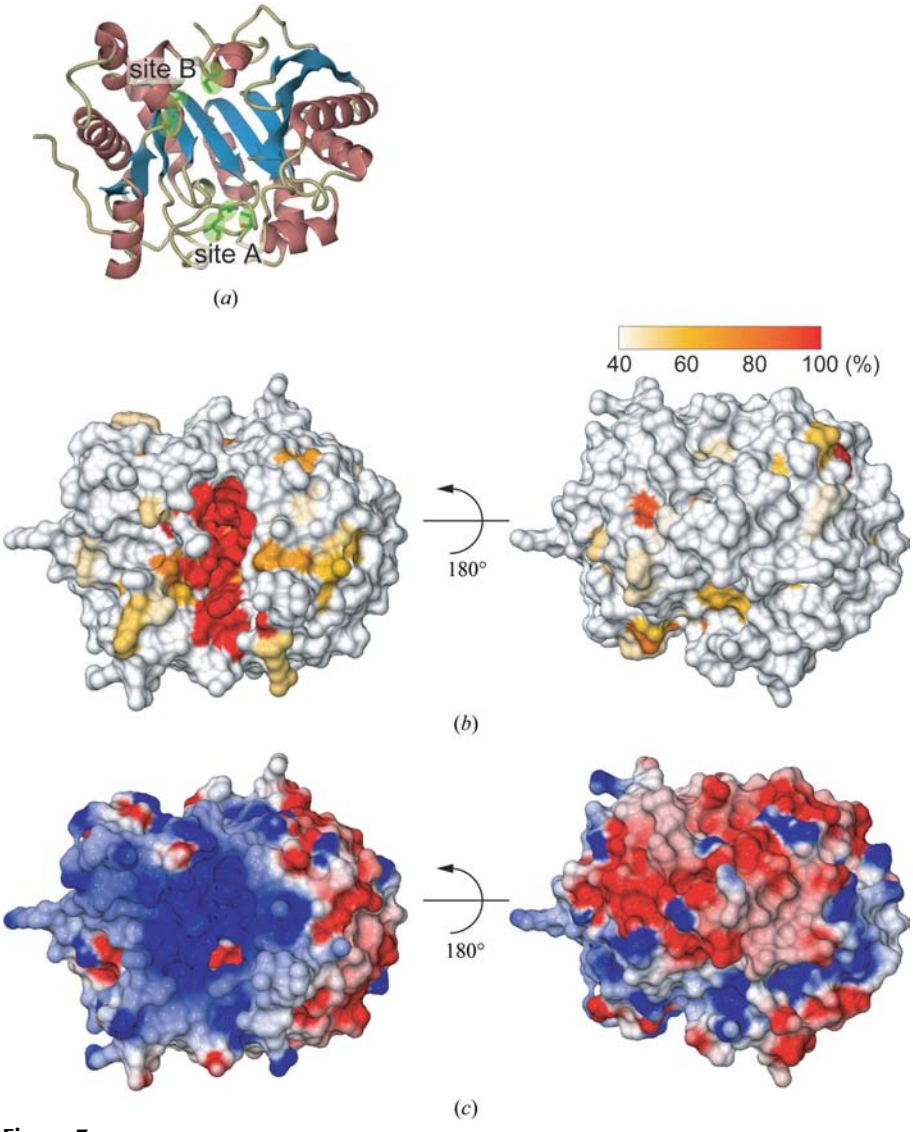

Figure 7
P. horikoshii TYW1 surface plots of the conservation rate and electrostatic potential. (*a*), (*b*) and (*c*) are shown on the same scale and from the same direction. (*a*) Ribbon diagram of *P. horikoshii* TYW1 with the cysteine residues comprising the FeS cluster sites in light green. (*b*) The conservation rate of the surface residues of *P. horikoshii* TYW1 is plotted onto its molecular surface and is depicted in a colour gradation from yellow (40% identity) to red (100% identity), as shown in the colour bar. Residues with conservation rates below 40% are coloured white. *ClustalX* was used for the calculation of the conservation rates and this and following surface models of *P. horikoshii* TYW1 were drawn with *MSMS*. (*c*) The electrostatic surface potential of *P. horikoshii* TYW1 was calculated with *GRASP* (Nicholls *et al.*, 1991). Positive and negative charges are shown in blue and red, respectively.

3.5. tRNA-binding ability of *P. horikoshii* TYW1

The complex structure of *P. horikoshii* TYW1 and tRNA with the FeS clusters, AdoMet and the two-carbon molecule will more precisely clarify the reaction mechanism. In preliminary experiments, we tested *P. horikoshii* TYW1 for its binding to tRNA. Unmodified *P. horikoshii* $tRNA^{Phe}_{GAA}$ was chosen as the candidate for the substrate. As shown in Fig. 9(*a*), binding of *P. horikoshii* TYW1 to the full-length *P. horikoshii* $tRNA^{Phe}_{GAA}$ transcript was observed. Furthermore, we tested the ability of *P. horikoshii* TYW1 to bind to the *M. jannaschii* $tRNA^{Phe}_{GAA}$ anticodon stem-loop. It should be noted that the sequence of the *M. jannaschii*

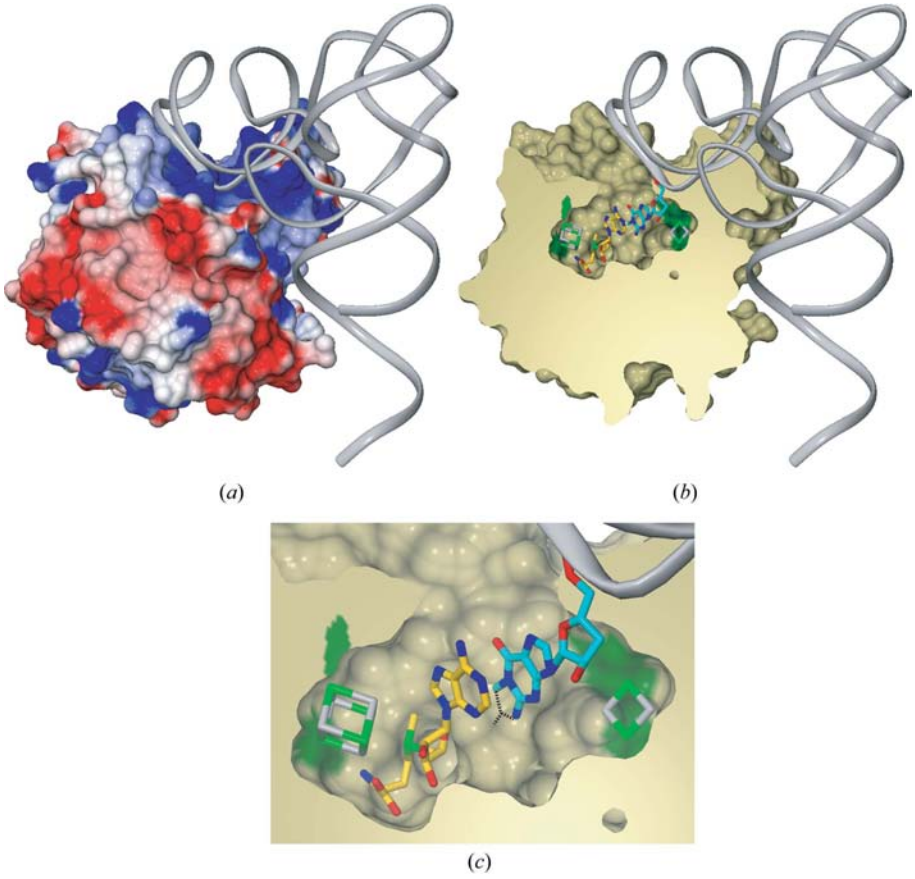

Figure 8
Docking model of *P. horikoshii* TYW1, FeS clusters, AdoMet and tRNA. (*a*) The overall docking model. *P. horikoshii* TYW1 is shown as a surface electrostatic potential model as in Fig. 7(*c*). The modelled tRNA is depicted by a grey ribbon. (*b*) A cross-section of (*a*). *P. horikoshii* TYW1 is shown as a beige surface model, with the cysteines comprising the FeS cluster site coloured green. The modelled FeS cluster, AdoMet and m^1G37 of tRNA are shown in stick models with grey and green, yellow and blue C atoms, respectively. (*c*) Close-up of (*b*). The dashed black lines show the hypothetical imG-14 structure to be formed.

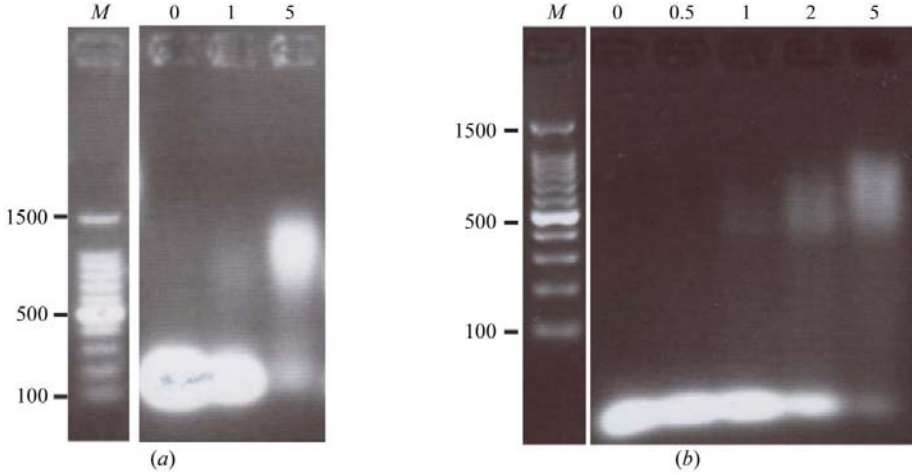

Figure 9
Binding assay of *P. horikoshii* TYW1 with full-length tRNA and the tRNA anticodon stem-loop. The binding of *P. horikoshii* TYW1 with (*a*) the full-length tRNA and (*b*) the tRNA anticodon stem-loop was monitored by gel-mobility shift assays. Lane *M* contains DNA size markers (labelled in bp). *P. horikoshii* TYW1 and the tRNAs were mixed in various ratios and analyzed with a 2% agarose gel; the tRNA was stained with ethidium bromide. The numbers at the top of the lanes correspond to the [TYW1]/[RNA] molar ratio.

$tRNA^{Phe}_{GAA}$ anticodon stem-loop is similar to that of the *P. horikoshii* $tRNA^{Phe}_{GAA}$ anticodon stem-loop, with the only substitution being of a U–A base pair in the stem in *M. jannaschii* by a C–G base pair in *P. horikoshii*. We found that the *M. jannaschii* $tRNA^{Phe}_{GAA}$ anticodon stem-loop alone bound to *P. horikoshii* TYW1 with a similar affinity as with the full-length tRNA (Fig. 9*b*), which shows that the tRNA anticodon stem-loop is sufficient for recognition by *P. horikoshii* TYW1.

We thank Dr Henri Grosjean for fruitful discussions. We thank Mr H. Sasaki for kindly providing us with purified *P. horikoshii* $tRNA^{Phe}_{GAA}$ and Dr T. Yanagisawa for his help in data collection. We are grateful to the staff at beamlines BL5 and NW12A of the Photon Factory for their support during data collection. This work was supported by the RIKEN Structural Genomics/Proteomics Initiative (RSGI), the National Project on Protein Structural and Functional Analyses, Ministry of Education, Culture, Sports, Science and Technology of Japan.

References

Adams, P. D., Pannu, N. S., Read, R. J. & Brünger, A. T. (1997). *Proc. Natl Acad. Sci. USA*, **94**, 5018–5023.
Berkovitch, F., Nicolet, Y., Wan, J. T., Jarrett, J. T. & Drennan, C. L. (2004). *Science*, **303**, 76–79.
Blobstein, S. H., Grunberger, D., Weinstein, I. B. & Nakanishi, K. (1973). *Biochemistry*, **12**, 188–193.
Grosjean, H. (2005). Editor. *Fine-Tuning of RNA Modifications and Editing.* Berlin/Heidelberg: Springer-Verlag.
Hanzelmann, P. & Schindelin, H. (2004). *Proc. Natl Acad. Sci. USA*, **101**, 12870–12875.
Hatfield, D., Feng, Y. X., Lee, B. J., Rein, A., Levin, J. G. & Oroszlan, S. (1989). *Virology*, **173**, 736–742.
Konevega, A. L., Soboleva, N. G., Makhno, V. I., Semenkov, Y. P., Wintermeyer, W., Rodnina, M. V. & Katunin, V. I. (2004). *RNA*, **10**, 90–101.
Kuchino, Y., Borek, E., Grunberger, D., Mushinski, J. F. & Nishimura, S. (1982). *Nucleic Acids Res.* **10**, 6421–6432.
La Fortelle, E. de & Bricogne, G. (1997). *Methods Enzymol.* **276**, 472–494.
Layer, G., Heinz, D. W., Jahn, D. & Schubert, W. D. (2004). *Curr. Opin. Chem. Biol.* **8**, 468–476.

Layer, G., Moser, J., Heinz, D. W., Jahn, D. & Schubert, W. D. (2003). *EMBO J.* **22**, 6214–6224.
Lepore, B. W., Ruzicka, F. J., Frey, P. A. & Ringe, D. (2005). *Proc. Natl Acad. Sci. USA*, **102**, 13819–13824.
Li, J., Esberg, B., Curran, J. F. & Bjork, G. R. (1997). *J. Mol. Biol.* **271**, 209–221.
McCloskey, J. A., Graham, D. E., Zhou, S., Crain, P. F., Ibba, M., Konisky, J., Soll, D. & Olsen, G. J. (2001). *Nucleic Acids Res.* **29**, 4699–4706.
Motorin, Y. & Grosjean, H. (2001). *Encyclopedia of Life Sciences*, pp. 1–9. New York: Wiley.
Murphy, F. V. IV, Ramakrishnan, V., Malkiewicz, A. & Agris, P. F. (2004). *Nature Struct. Mol. Biol.* **11**, 1186–1191.
Murshudov, G. N., Vagin, A. A. & Dodson, E. J. (1997). *Acta Cryst.* D**53**, 240–255.
Nicholls, A., Sharp, K. A. & Honig, B. (1991). *Proteins*, **11**, 281–296.
Noma, A., Kirino, Y., Ikeuchi, Y. & Suzuki, T. (2006). *EMBO J.* **25**, 2142–2154.
Noon, K. R., Guymon, R., Crain, P. F., McCloskey, J. A., Thomm, M., Lim, J. & Cavicchioli, R. (2003). *J. Bacteriol.* **185**, 5483–5490.
Otwinowski, Z. & Minor, W. (1997). *Methods Enzymol.* **276**, 307–326.
Schneider, T. R. & Sheldrick, G. M. (2002). *Acta Cryst.* D**58**, 1772–1779.
Smith, C., Schmidt, P. G., Petsch, J. & Agris, P. F. (1985). *Biochemistry*, **24**, 1434–1440.
Terwilliger, T. C. (2000). *Acta Cryst.* D**56**, 965–972.
Ugulava, N. B., Gibney, B. R. & Jarrett, J. T. (2001). *Biochemistry*, **40**, 8343–8351.
Urbonavicius, J., Qian, Q., Durand, J. M., Hagervall, T. G. & Bjork, G. R. (2001). *EMBO J.* **20**, 4863–4873.
Vagin, A. & Teplyakov, A. (1997). *J. Appl. Cryst.* **30**, 1022–1025.
Vonrhein, C., Blanc, E., Roversi, P. & Bricogne, G. (2006). *Macromolecular Crystallography Protocols*, Vol. 2, *Structure Determination*, edited by S. Doublié, pp. 215–230. Totowa, NJ, USA: Humana Press.
Waas, W. F., de Crecy-Lagard, V. & Schimmel, P. (2005). *J. Biol. Chem.* **280**, 37616–37622.
Yarian, C., Townsend, H., Czestkowski, W., Sochacka, E., Malkiewicz, A. J., Guenther, R., Miskiewicz, A. & Agris, P. F. (2002). *J. Biol. Chem.* **277**, 16391–16395.
Zhou, S., Sitaramaiah, D., Noon, K. R., Guymon, R., Hashizume, T. & McCloskey, J. A. (2004). *Bioorg. Chem.* **32**, 82–91.